

Review

# Integrated Resonant Micro/Nano Gravimetric Sensors for Bio/Chemical Detection in Air and Liquid

Hao Jia , Pengcheng Xu and Xinxin Li \*

State Key Lab of Transducer Technology, Shanghai Institute of Microsystem & Information Technology, Chinese Academy of Sciences, 865 Changning Road, Shanghai 200050, China; hao.jia@mail.sim.ac.cn (H.J.); xpc@mail.sim.ac.cn (P.X.)

\* Correspondence: xxli@mail.sim.ac.cn

**Abstract:** Resonant micro/nanoelectromechanical systems (MEMS/NEMS) with on-chip integrated excitation and readout components, exhibit exquisite gravimetric sensitivities which have greatly advanced the bio/chemical sensor technologies in the past two decades. This paper reviews the development of integrated MEMS/NEMS resonators for bio/chemical sensing applications mainly in air and liquid. Different vibrational modes (bending, torsional, in-plane, and extensional modes) have been exploited to enhance the quality ( $Q$ ) factors and mass sensing performance in viscous media. Such resonant mass sensors have shown great potential in detecting many kinds of trace analytes in gas and liquid phases, such as chemical vapors, volatile organic compounds, pollutant gases, bacteria, biomarkers, and DNA. The integrated MEMS/NEMS mass sensors will continuously push the detection limit of trace bio/chemical molecules and bring a better understanding of gas/nanomaterial interaction and molecular binding mechanisms.

**Keywords:** integrated resonators; gravimetric sensors; bio/chemical sensing; quality factor; resonant modes



**Citation:** Jia, H.; Xu, P.; Li, X. Integrated Resonant Micro/Nano Gravimetric Sensors for Bio/Chemical Detection in Air and Liquid. *Micromachines* **2021**, *12*, 645. <https://doi.org/10.3390/mi12060645>

Academic Editor: Frederic Nabki

Received: 7 May 2021  
Accepted: 27 May 2021  
Published: 31 May 2021

**Publisher's Note:** MDPI stays neutral with regard to jurisdictional claims in published maps and institutional affiliations.



**Copyright:** © 2021 by the authors. Licensee MDPI, Basel, Switzerland. This article is an open access article distributed under the terms and conditions of the Creative Commons Attribution (CC BY) license (<https://creativecommons.org/licenses/by/4.0/>).

## 1. Introduction

The past two decades have witnessed significant development in sensor technologies for the recognition and detection of chemical (e.g., volatile organic compounds, VOCs) and biological species (e.g., cells, proteins) in ambient and liquid environments. In contrast to the optical methods, micro-/nanoelectromechanical systems (e.g., microcantilevers), featured by miniature device size, exquisite detection limit (from part per million to part per trillion, or micromolar to femtomolar), and easy to be on-chip integrated, have offered better opportunities to detect the trace analytes and capture the molecular interaction processes in gas and liquid phases [1–3].

Taking the prevailing microcantilever sensors as an example, two different operational modes (i.e., static and dynamic modes) have been engineered for bio/chemical sensing. In static mode, the cantilever surface is functionalized to have a good affinity to the target molecules. The stress change at the cantilever surface (owing to electrostatic repulsion or attraction, steric interactions, hydration, and entropic effects) causes the cantilever bending, which is usually measured by an optical lever system [4]. Since the responses of surface-stress sensors are difficult to interpret, a dynamic scheme has been proposed by operating a cantilever at resonance. A tiny mass loading ( $\Delta m$ ) at a cantilever free end can lead to a resonant frequency downshift ( $\Delta f$ ), which defines the mass sensitivity:  $\mathfrak{R} = \Delta f / \Delta m = -f / 2M$ , where  $f = 1 / 2\pi \sqrt{k / M}$  is the resonant frequency,  $k$  and  $M$  are the effective spring constant and effective mass of the resonant device [5]. Therefore, one can perceive that micro- and nanoelectromechanical (MEMS/NEMS) resonators promise gravimetric detection of trace analytes down to a fraction of the sensor mass. In comparison with the conventional quartz crystal microbalances (QCM), the silicon micro-machined resonant cantilevers possess finer mass resolution, smaller size, low-cost batch fabrication, and

easy IC-compatible integration [6]. Although pioneering efforts have been made towards attogram and atomic-level resonant mass sensing, with outstanding device performance often achieved by off-sensor optical detection methods in high vacuum or at low temperature [7–16], there is an increasing need for portable micro- and nano-gravimetric sensors with integrated resonance excitation and readout elements on-chip, toward real-world bio/chemical sensing applications.

To date, several on-chip resonance excitation and readout mechanisms have been developed, considering their compatibility with ambient and liquid conditions (especially conductive biosolutions). As to resonance readout, most microcantilevers use piezoresistive effect, as the doped semiconducting materials (mostly silicon) provide very large gauge factors, and the fabrication process has been well-developed and optimized [17,18]. The piezoresistors are often patterned at the device's clamping points (e.g., fixed end of the cantilever), where the largest stress is expected at resonance. Wheatstone bridge with 4 terminal piezoresistors is also desirable to improve the displacement sensitivity to nanometer scale in air and liquid.

As to resonance excitation, electrothermal excitation has been widely adopted on many resonant MEMS/NEMS prototypes, such as microcantilevers [19], 'dog-bone' resonators [20], and disk resonators [21]. A DC + AC voltage signal is typically applied to a heating resistor patterned at the device's clamping points, and the time-varying heating power whose cycle matches the device's resonant frequency induces the mechanical vibration. On the other hand, electromagnetic excitation has been achieved with metal loops patterned around the cantilevers. With the presence of an external magnetic field (tens of mT) and an AC electrical current flowing through the metal loops, Lorentzian force drives the bending or torsional vibration, depending on the positions of the metal loops on the resonators [17,22].

Alternatively, the piezoelectric approach emerges with the successful synthesis of ceramics with high piezoelectric constants (such as aluminum nitride, AlN, Pb-based lanthanum-doped zirconate titanates, PZT). The piezoelectric effect enables simultaneous self-excitation/readout. A pure AC input signal creates time-varying stress at the clamping points, while another AC piezoelectric current signal is generated to read out the resonant frequency [23–25].

Although on-chip, all-electrical integration brings immense simplification to the bulky, expensive measurement system that is inevitable for optical readout, researchers are still confronted with technical challenges of operating resonant sensors in viscous media that dissipates resonating energy, and great endeavors have been made to achieve better device performance (e.g., higher  $Q$ , better mass sensitivity and mass resolution) in air and liquid by studying different vibrational modes, such as bending, torsional, in-plane, and extensional modes (as shown in Figure 1 and Table 1).

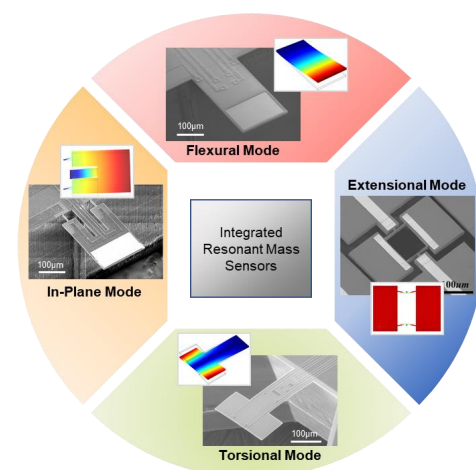


**Figure 1.** Integrated resonant gravimetric sensors using different vibrational modes, such as bending,

torsional, in-plane, and extensional modes. Reprinted with permission from [17,19,20,26]. Copyright 2007 American Institute of Physics, 2019 Royal Society of Chemistry, 2016 IEEE, 2011 Elsevier B.V.

**Table 1.** Performance of typical integrated resonant gravimetric sensors in air using different vibrational modes.

Devices	Resonant Frequency	Q Factor	Sensing Performance		Refs
Fundamental Bending-Mode Cantilevers	47.838 kHz	168	0.43 Hz/pg	0.26 pg	[27]
High-Order Bending-Mode Cantilevers	298.132 kHz	867	2.7 Hz/pg	30 fg	[27]
Torsional-Mode Cantilevers	114.805 kHz	252	0.9 Hz/pg	23 fg	[28]
High-Order Torsional-Mode Cantilevers	508.082 kHz	286	5.1 Hz/pg	9 fg	[28]
In-Plane Mode Cantilevers	536 kHz	2096	/	/	[26]
Extensional-Mode Resonators	4.1 MHz	11157	10.617 Hz/pg	0.94 pg	[29]

## 2. Integrated Resonant Gravimetric Sensors Using Different Vibrational Modes

### 2.1. Integrated Resonant Gravimetric Sensors Using Fundamental Bending Modes

Microcantilever vibrating at its fundamental bending mode is the most common type of resonant mass sensor. Figure 2b shows a typical cantilever mass sensor with integrated thermoelectric excitation and Wheatstone bridge readout components [18]. As illustrated in Figure 2a, 4 piezoresistors and 1 heating resistor near the fixed end of the cantilever are created by boron-doping through thermally grown silicon oxide (SiO<sub>2</sub>) windows. With patterned aluminum interconnects covered by PECVD SiO<sub>2</sub> passivation layer and Au/Cr sensing pad at the free end, the cantilever is finally released by the backside deep reactive ion etching (DRIE), followed by the removal of SiO<sub>2</sub> by hydrofluoric acid (HF). The heating power with a DC + AC voltage is given by  $P = (V_{DC} + V_{AC} \cos \omega t)^2 / R$ , where  $R$  is the resistance of the piezoresistive heater,  $\omega = 2\pi f$ , where  $f$  is the driving frequency. One can perceive that the mechanical resonance is excited by the  $V_{DC} \cdot V_{AC} \cos \omega t / R$  component (given that  $V_{DC} \gg V_{AC}$ ). The sensing region at the cantilever free end is covered by an Au film for subsequent chemical functionalization. Such resonant cantilevers with dimensions of  $200 \times 100 \times 3 \mu\text{m}$  have exhibited fundamental-mode resonant frequencies  $f \sim 100 \text{ kHz}$ , and quality factors  $Q > 100$ . With a mass sensitivity  $\sim 1.5 \text{ Hz/pg}$  and mass resolution  $\sim 0.1 \text{ pg}$ , various hazardous chemical vapors, e.g., Trinitrotoluene (TNT), dimethyl methyl phosphonate (DMMP), VOCs and biological species (e.g., bacteria, proteins, DNA) with very low concentrations have been successfully detected.

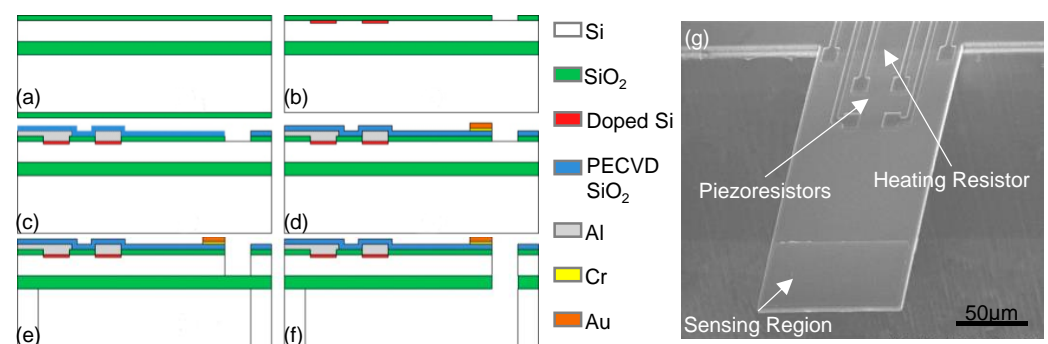


**Figure 2.** Bending-mode cantilever mass sensors. (a–f) Fabrication process of microcantilevers showing on-chip integration of electrothermal excitation and piezoresistive readout. (g) Typical resonant sensor with sensing region at the free end for nanomaterial loading. Reprinted with permission from [18]. Copyright 2009 IOP Publishing Ltd.

It is worth noting that with all-electrical integration, a resonator is readily connected to a phase-lock loop (PLL) for real-time frequency tracking. Hence, the minimum de-

tectable mass is defined by the minimum detectable phase change of the system, given by  $\delta m = (\delta\theta/Q)M$  [30]. Therefore, the mass resolution is significantly dependent on the  $Q$  factor, which is inevitably deteriorated by the strong viscous damping in air and liquid. Therefore, researchers have been exploring other high-order resonance modes to improve the  $Q$  factor and mass sensing performance.

## 2.2. Integrated Resonant Gravimetric Sensors Using Higher-Order Bending Modes

The enhancement in  $Q$  factor and mass sensing performance when using high-order flexural modes has been demonstrated in many cases [9,27,31–35]. Taking cantilever resonators in air as an example, a ~5-fold increase in  $Q$  factors, ~6-fold increase in mass sensitivity, and >8-fold improvement in mass resolution have been demonstrated using the 2nd-order bending mode than using fundamental mode (as shown in Table 1). The increase in mass sensitivity (from 0.43 to 2.7 Hz/pg) can be attributed to the higher resonant frequency of 2nd-order bending mode (~298 kHz), which is ~6-fold higher than that of the fundamental mode (~47.8 kHz). The improvement in  $Q$  factor (from 867 to 168) has been analyzed from the perspective of flow pattern over the width of the cantilever. Using finite element simulation, less energy dissipations into the viscous media have been visualized for high order bending modes, leading to higher  $Q$ s [28,36,37].

## 2.3. Integrated Resonant Gravimetric Sensors Using Torsional Modes

Torsional modes have also been exploited to improve the sensing performance of resonant mass sensors [17,22,28,38]. Figure 3b shows a typical T-shaped torsional-mode cantilever with on-chip integrated electromagnetic excitation and piezoresistive readout components [17]. The fabrication process of torsional-mode resonators is similar to that of bending-mode resonators. 4 piezoresistors are formed by boron-doping using  $\text{SiO}_2$  mask. Aluminum is patterned not only as the interconnects but also as the metal loop for electromagnetic excitation. After the Cr/Au sensing pads are defined by liftoff, the device is released by both frontside RIE, backside DRIE, and  $\text{SiO}_2$  removal by HF. Together with a decent increase in  $Q$  factor, Xia et al. have reported a significant enhancement in mass sensing performance using torsional modes. The >10-fold increase in mass sensitivity is attributed to the much higher resonant frequencies of the torsional modes than that of the fundamental mode. Benefited from high-order torsional vibrations, the mass detection limit has been improved by almost 30 times, down to 9 fg in air [22].

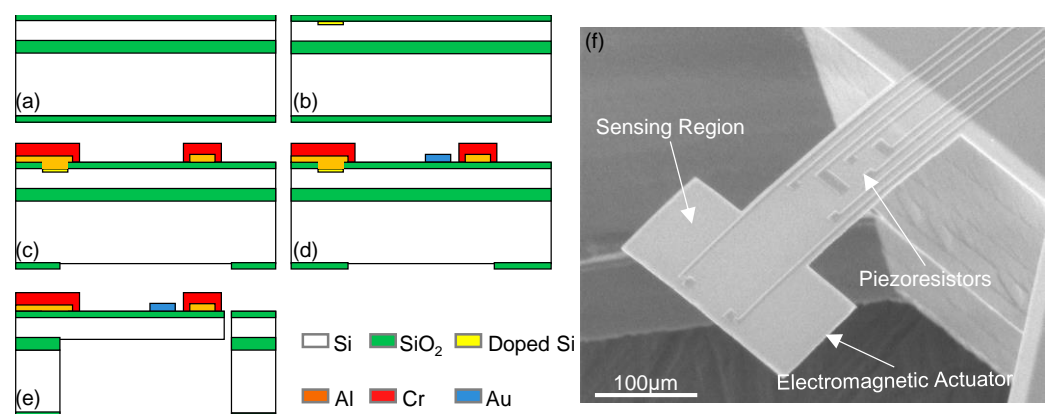


**Figure 3.** Torsional-mode cantilever mass sensors. (a–e) Fabrication process of the microcantilevers showing on-chip integration of electromagnetic excitation and piezoresistive readout. (f) Typical resonant sensor with 2 sensing regions for nanomaterial loading. Reprinted with permission from [17]. Copyright 2007 American Institute of Physics.

## 2.4. Integrated Resonant Gravimetric Sensors Using In-Plane Modes

Resonant gravimetric sensors using in-plane modes have been studied [26,39,40], as shown in Figure 4b. To achieve effective excitation and detection of in-plane vibration,

thin beam legs are doped to form resistors for electrothermal driving and piezoresistive readout. The fabrication process is similar to that for bending-mode cantilevers, as shown in Figure 4a. An additional oxygen annealing step is often performed to protect the vertical sidewalls of the cantilever and tiny beams against electric leakage in conductive solutions since these devices are often designed for bio/chemical sensing in liquid. An important merit of using in-plane mode is the high  $Q$  factors  $>2000$  in air, which is  $>10$ -fold better than that of the fundamental mode (as shown in Table 1). As this type of resonator is often used for biosensing applications in liquid, the sensing performance will be detailed in Section 3.3.

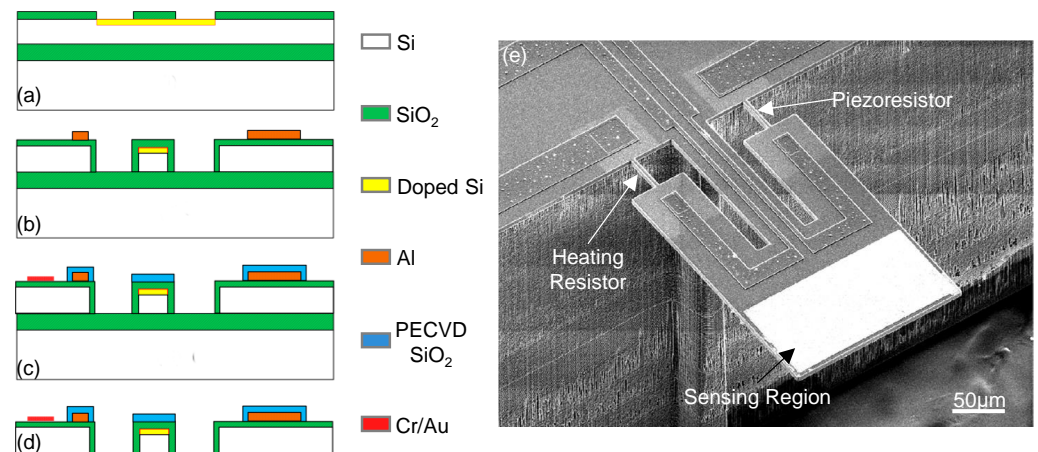


**Figure 4.** In-plane-mode resonant microcantilever mass sensors. (a–d) Fabrication process of microcantilevers showing on-chip integration of electrothermal excitation and piezoresistive readout. (e) Typical resonant sensor with sensing region for loading functional nanomaterials. Reprinted with permission from [26]. Copyright 2011 Elsevier B.V.

### 2.5. Integrated Resonant Gravimetric Sensors Using Extensional Modes

Extensional-mode resonators typically have ‘dog-bone’ structure [20,29,41], which is quite different from a cantilever, as shown in Figure 5. Two large sensing pads are connected by 2 or 3 thin beams and vibrate oppositely along the device length. The piezoresistive arms are designed for electrothermal excitation and piezoresistive readout of the extensional mode. The fabrication process of the ‘dog-bone’ resonator is quite similar to that of in-plane mode cantilevers. Such mass sensors using bulk mode surpass the aforementioned bending, torsional, and in-plane mode resonators in terms of  $Q$  factor and mass sensitivity.  $Q$  factors  $> 11,000$  and mass sensitivity up to  $10.6$  Hz/pg have been reported, which are  $\sim 65$ -time and  $\sim 25$ -time higher than those from fundamental-mode cantilevers (refer to Table 1).

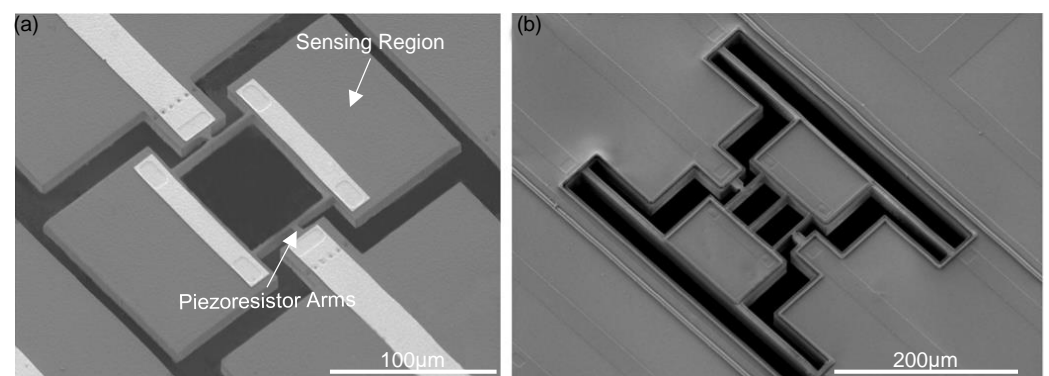


**Figure 5.** Extensional-mode ‘dog-bone’ mass sensors. (a,b) Two types of devices with sensing pads connected by dual- and tri-beams. Reprinted with permission from [20]. Copyright 2016 IEEE.

Overall, resonant mass sensors, with integrated excitation and readout schemes and enhanced mass sensing performance by different vibrational modes, have opened up new possibilities for ultrasensitive bio/chemical detection in gas- and liquid phases, which will be detailed in the following section.

### 3. Integrated Resonant Gravimetric Sensors for Bio/Chemical Detection

#### 3.1. Integrated Resonant Gravimetric Sensors for Gas Detection

The ability to detect trace chemical vapors (e.g., TNT, DMMP), VOCs (e.g., aniline, xylene), and other pollutant gases (e.g., carbon monoxide, CO, sulfur oxide, SO<sub>2</sub>) is highly demanded in environmental protection, industrial pollution control, biomedical systems, and public safety. However, the very low concentration of target gases, interfering gases, and potable sensor design have imposed great challenges in on-the-spot, rapid detection. Therefore, great attention has been made to engineer integrated resonant gravimetric sensors for gas sensing, thanks to their small size, ultra-high sensitivity, and scalability for mass production.

Figure 6a shows an example of a cantilever gas sensor, with nanomaterials (hexafluoro-2-propanol-functionalized mesoporous silica, HFMS, shown in the inset) loaded to the sensing region near the free end [42]. The cantilever is electrothermally excited at its fundamental mode, and the resonant frequency is monitored in real-time using PLL control. When the target gas molecules flow over the cantilever (e.g., 45 ppt, 90 ppt, 135 ppt TNT in Figure 6b), the molecules are adsorbed onto the nanomaterials, hence decrease the resonant frequency. The presence of functionalized nanomaterials can greatly improve the sensor selectivity of the target gas. As shown in Figure 6c, the HFMS-based cantilever resonator is highly responsive to TNT than other interference gases.

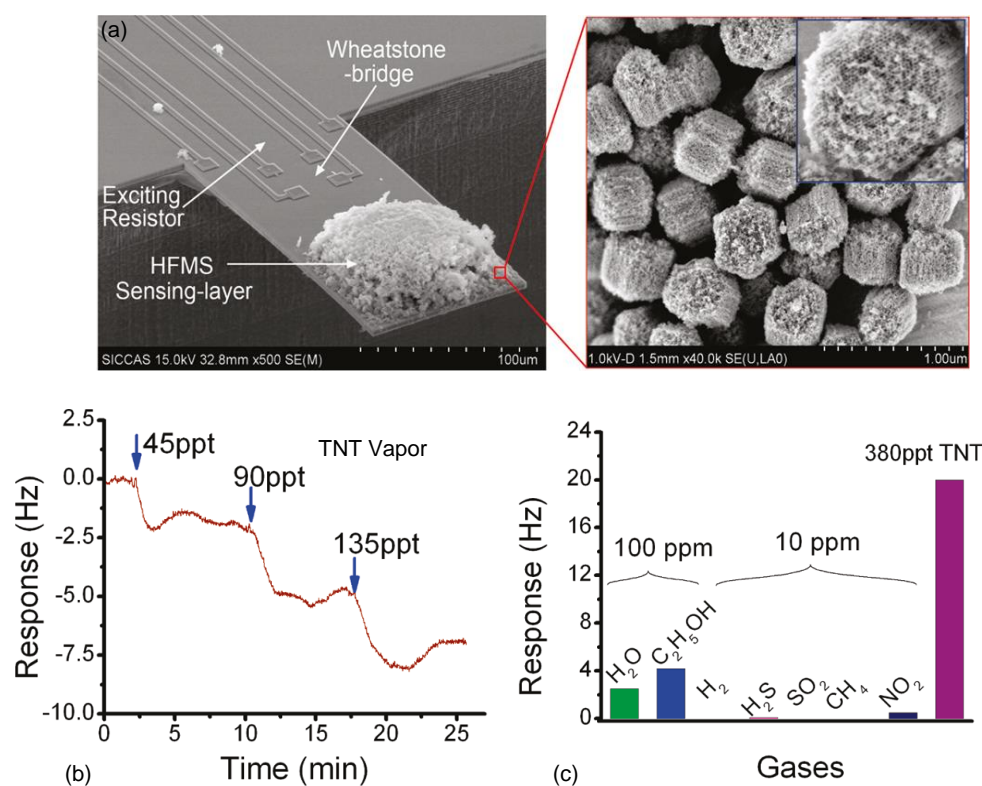


**Figure 6.** TNT vapor detection using a microcantilever sensor. (a) SEM images showing a microcantilever sensor with loaded HEMS nanomaterials. (b) Frequency responses of the microcantilever to TNT vapors at different concentrations. (c) Sensor responses to various kinds of interfering gases compared with 380 ppt TNT vapor. Reprinted with permission from [42]. Copyright 2011 American Chemical Society.

So far, resonant cantilever sensors have shown great potential in detecting many kinds of trace analytes, such as chemical vapors, VOCs, and pollutant gases, as summarized in Table 2. In general, the cantilever mass sensors exhibit detection limits from ~100 pb to ~10 ppt level for detecting chemical vapors, such as TNT, DMMA, TMA. The detection limit for VOCs falls in ~1 ppm–100 ppb level, such as aniline, xylene. As to pollutant gases, such as CO, SO<sub>2</sub>, the minimum detectable concentrations as low as ~10 ppb have been demonstrated. The cantilever resonators also promise fast response time from tens of seconds to ~10 min, thanks to the optimized design of resonators and nanomaterials.

**Table 2.** Integrated Resonant Gravimetric Sensors for Gas Sensing.

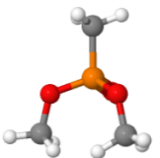
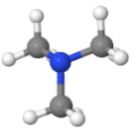
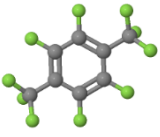
Targets	Sensing Materials	Gas Sensing Performance		Refs
 TNT Vapor	HFIP-MWCNTs	~1.2 ppb	~5 min	[43]
	HFIP-Mesoporous Silica	~20.8 ppt	~2 min	[42]
	HFIP-GO/Au-NPs hybrid	~60 ppt	~1 min	[44]
 DMMP Vapor	Siloxane-Hyperbranched Polymers	~5 ppb	~3 min	[18]
	Mesoporous Silica Nanoparticles	<1 ppb	<6 min	[45]
	HB-PCSOX-BHPHFB	<300 ppb	5 min	[46]
	BHPF-KIT-5 Mesoporous Silica	~30 ppb	~10 min	[47]
	UiO-66 film	<5 ppb	~10 min	[19]
 TMA Vapor	–COOH-Mesoporous Silica	~0.8 ppm	~6 min	[48]
	AuNP-rGO	~0.5 ppm	<30 s	[49]
 NH <sub>3</sub> Gas	–COOH-Au-NPs/rGO	<10 ppm	~5 min	[50]
	Carboxyl- Mesoporous Silica Nanoparticles	<5 ppb	~1.8 min	[51]
 Aniline Vapor	MOF-5	<1.4 ppm	~1.8 min	[52]
 p-xylene	HKUST-1	~120 ppb	~15 min	[53]

Table 2. Cont.

Targets	Sensing Materials	Gas Sensing Performance		Refs
 CO	Ni-MOF-74	<10 ppb	~5 min	[54]
 SO <sub>2</sub>	ZnO Nanowires	~70 ppb	~10 min	[55]
 CO <sub>2</sub> Gas	-NH <sub>2</sub> -MTF	30 ppm	<60 s	[56]

### 3.2. Integrated Resonant Gravimetric Sensors for Biosensing in Air

The detection of biological species, such as bacteria, viruses, and proteins is of great importance for disease diagnosis, food safety, and fundamental research. Luckily, some of these species can survive in humid air, hence they can be detected by resonant mass sensors. In these cases, the resonators are operated in ‘dip-and-dry’ mode, without suffering from strong viscous damping. After sufficient time for immobilization of bacteria or antigen-antibody interactions in solution, the resonators are dried, and the resonant frequencies before and after dipping are recorded.

Using such an approach, Xu et al. have reported the detection of *Escherichia coli* (*E. coli*) O157:H7 down to 10<sup>3</sup> CFU/mL, and *Bacillus Anthracis* as low as 10<sup>3</sup> spores/mL using cantilever mass sensors [57]. With an ultra-high mass resolution down to 9 fg, Xia et al. have demonstrated the detection of 60 ng/mL alpha-fetoprotein (AFP) using torsional-mode resonators [22].

### 3.3. Resonant Gravimetric Sensors for Bio/Chemical Detection in Liquid

Although the ‘dip-and-dry’ method has been proved to be effective for certain cases that avert device immersion in liquid, direct sensing in liquid is highly desirable, especially for biological applications since most biological processes take place in liquid. The much stronger viscous damping in liquid than in air has imposed great challenges in detecting trace bio/chemical analytes in liquid using resonant gravimetric sensors. For example, fundamental-mode cantilever resonators typically exhibit  $Q_s$  ~10–20 when operated in liquid (e.g., water, phosphate buffered saline, PBS) (refer to Table 3). Still, prostate-specific antigen (PSA), C-reactive protein (CRP), DNA with concentrations between 10 µg/mL to 10 ng/mL are detectable using such gravimetric sensors.

Several approaches have been taken to improve the sensing performance of resonant mass sensors in liquid. First, as mentioned in Section 2,  $Q$  factor and mass sensitivity can be improved by exploiting vibrational modes beyond fundamental mode. Figure 7 shows an example of monitoring heavy metal-ion (Hg<sup>2+</sup>) in water (mimicking ion pollution to water resource) using extensional-mode ‘dog-bone’ resonators [20].  $Q$  factor ~256 and mass sensitivity ~9.76 Hz/pg have been observed, which are >10-time and ~100-time higher than those of fundamental-mode cantilevers. With -SH modified mesoporous silica loaded to the sensing regions, 500 ppb Hg<sup>2+</sup> can be easily discerned from frequency response (as shown in Figure 7b). Second, new device structures can be engineered to isolate the resonators from strong liquid damping. For example, suspended microchannel resonators, SMRs [58–64], have drawn considerable attention because of their unique way of minimizing viscous damping by fabricating fluidic channels inside the cantilevers. Therefore, these devices are operated in vacuum, allowing ultra-high  $Q_s$  on the order of 1000–10,000, and unprecedented mass resolutions < 1 ag. Although this type of device has yet been on-chip fully integrated (resonances are often excited by off-chip piezoshaker, and detected by optical lever), and shown limitations in cases, for example, monitoring

adherent mass rather than floating mass, they still hold the records for mass sensing in liquid using cantilevers.

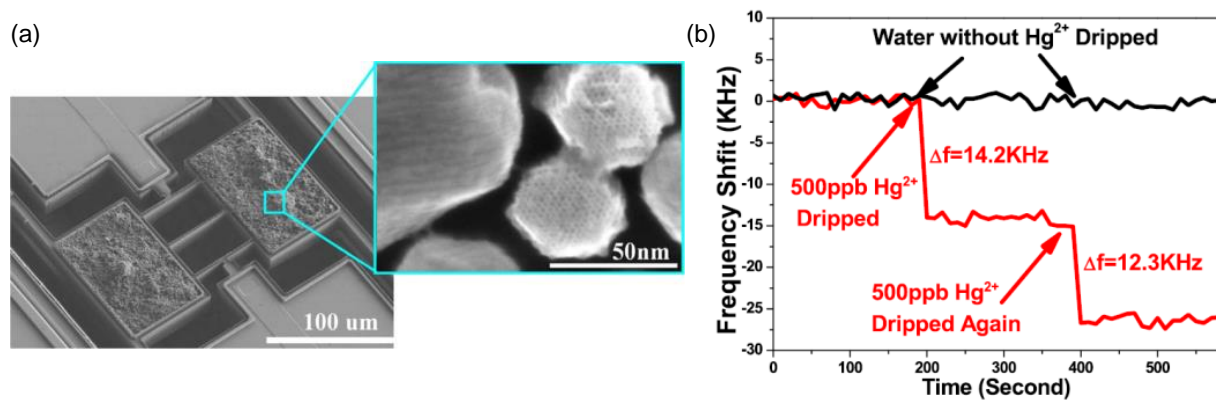


**Figure 7.** Detection of  $\text{Hg}^{2+}$  in liquid droplets using a tri-beam extensional-mode resonator. (a) SEM images showing a microcantilever sensor with loaded mesoporous silica. (b) Frequency responses of the resonator to 500 ppb and 1 ppm  $\text{Hg}^{2+}$  ion in solution. Reprinted with permission from [20]. Copyright 2016 IEEE.

**Table 3.** Integrated Resonant Microgravimetric Sensors for Biological Detection in Liquid.

Device	Dimensions	$f$	$Q$		Sensing Performance	Refs
PZT cantilever	$300 \times 100 \times 0.65 \mu\text{m}$	30.95 kHz	-	-	1–100 ng/mL PSA	[23]
Si Cantilever	$150 \times 140 \times 8.2 \mu\text{m}$	200 kHz	10	0.02 Hz/pg	10–100 ng/mL PSA	[67]
PZT Cantilever	$500 \times 500 \times 35 \mu\text{m}$	36.11 kHz	15–25	0.118 Hz/pg	10 $\mu\text{g}$ /mL CRP	[24]
Si Cantilever	$150 \times 140 \times 8.2 \mu\text{m}$	250 kHz	20	0.1 Hz/pg	10–100 ng/mL PSA	[68]
PZT Cantilever	$500 \times 500 \times 32 \mu\text{m}$	59 kHz	20	-	100 ng/mL CRP 5 $\mu\text{M}$ ssDNA	[25]
In-Plane Mode Cantilever	$190 \times 310 \times 5 \mu\text{m}$	406 kHz	14	8.8 Hz/pg	$2 \times 10^3$ CFU/mL <i>E. Coli</i> EcoRV-enzyme digestion of dsDNA	[26,39]
Rotational Disk	$d = 500 \mu\text{m}$	3.44 MHz	20–80	-	Hybridization between ssDNA (1.0 $\mu\text{M}$ ) and HS-ssDNA (2.0 $\mu\text{M}$ )	[21]
Encased Bending-Mode Cantilever	$200 \times 100 \times 3 \mu\text{m}$	50.615 kHz	23	-	$10^2$ CFU/mL <i>E. Coli</i>	[65]
Encased In-Plane Mode Cantilever	$190 \times 310 \times 3.7 \mu\text{m}$	576 kHz	208	1.23 Hz/pg	1–10 $\mu\text{M}$ ATP-Aptamer Interaction	[66]

Alternatively, resonant mass sensors can be directly immersed in liquid with decent  $Q$ s with the help of hydrophobic shells. Such a sensor platform is more suitable for measuring adherent masses, such as adherent cells and molecular binding. Yu et al. have shown the detection of *E. coli* down to  $10^2$  CFU/mL using a parylene-shell encased bending-mode cantilevers [65]. More recently, Wang et al. have extended such a technique to in-plane cantilevers [66].  $Q$  factor has been significantly improved to  $>200$ , and mass sensitivity has increased to 1.2 Hz/pg. Both are one order of magnitude better than conventional bending-mode cantilevers (refer to Table 3).

#### 4. NEMS Resonators for Ultrasensitive Gravimetric Sensing

To continuously pushing the detection limit of the integrated mass sensors, the device sizes have been miniaturized to the nanoscale. For example, nanobeams, nanowires, and

nanotubes have shown effective masses reduced by orders of magnitude to attogram. Subsequently, the resonance frequencies have increased by orders of magnitude up to 1 GHz. These devices have been used for atomic and molecular level mass sensing in vacuum, e.g., Au [8], Xe [12,69], Cr [14] atoms,  $C_{10}H_8$  molecule [16], bovine serum albumin (BSA), and  $\beta$ -amylase [15].

However, it worth noting that the limit of detection at single-molecule/atom level has been achieved through operating those NEMS resonators at very-high/ultra-high frequency (VHF/UHF) bands, but in stringent experimental conditions (e.g., high vacuum and low temperature). Meanwhile, the quality ( $Q$ ) factor decreases as the device sizes get smaller, which is due to the increased energy dissipation at the nanoscale than at the microscale.

Some mass sensing attempts have been made with nanocantilevers in air (as shown in Figure 8), which indeed show exquisite gravimetric sensitivities down to  $\sim 0.7$  Hz/zg and mass resolution  $\sim 0.1$  ag [70,71]. More attention still needs to be made to tackle the challenges of detecting VHF/UHF resonances with picometer displacement sensitivity while maintaining sufficient sensing area and decent  $Q$ s factors in air and liquid, such that the NEMS resonators can be widely used for bio/chemical sensing applications in gas and liquid-phases.

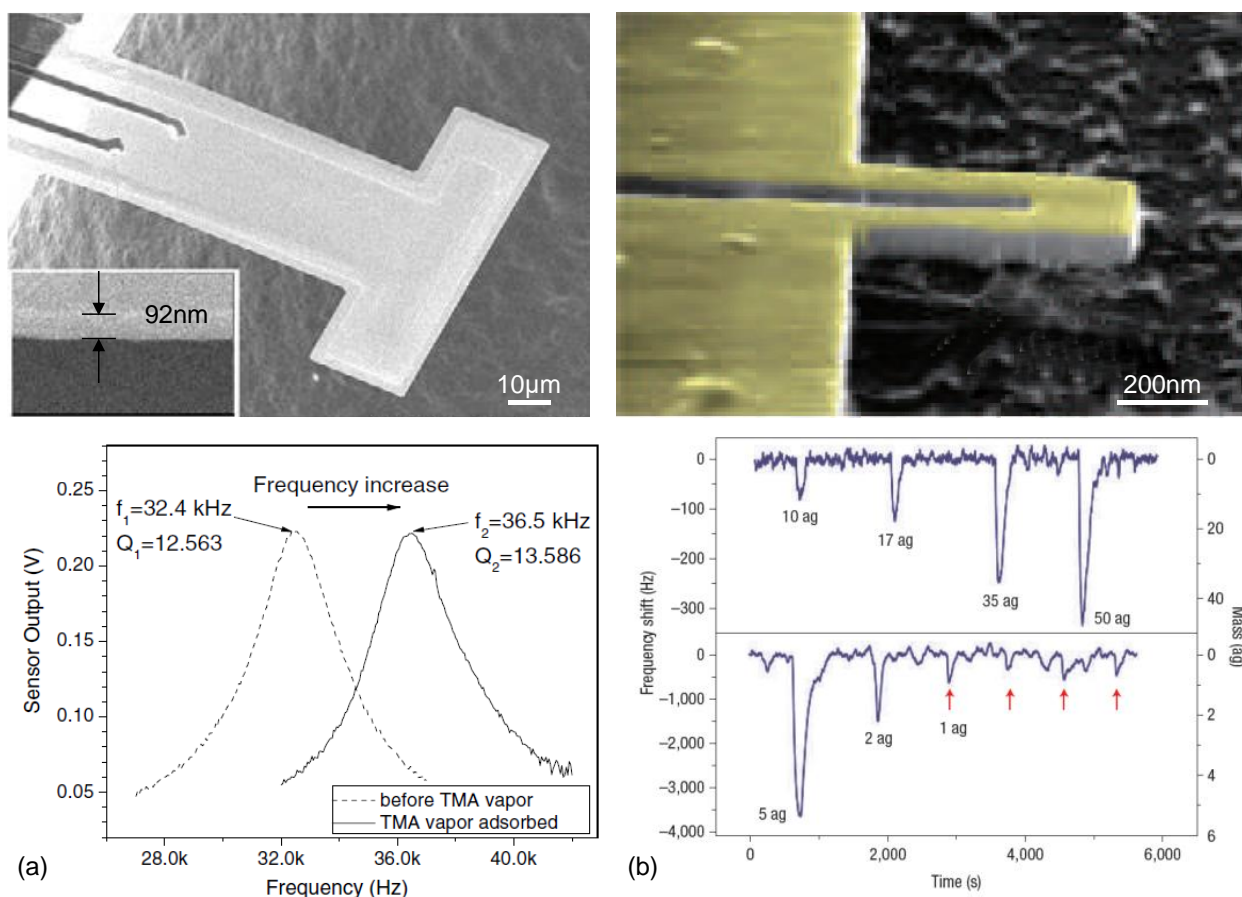


**Figure 8.** NEMS cantilevers for ultrasensitive gravimetric detection in air. (a) A T-shaped nano-thick cantilever with torsional resonant mode  $\sim 37.65$  kHz exhibits mass sensitivity  $\sim 860$  Hz/pg, and TMA detection limit  $< 0.1$  ppm. (b) A SiC nano cantilever with fundamental bending mode in the VHF band (up to 127 MHz), exhibits mass sensitivity  $\sim 0.7$  Hz/zg, and mass resolution  $\sim 0.1$  ag. Reprinted with permission from [70,71]. Copyright 2007 Nature Publishing Group, 2010 IOP Publishing Ltd.

## 5. Conclusions

This paper reviews the development of integrated resonant gravimetric resonators for bio/chemical sensing applications in the past two decades. Bending-, torsional-, in-plane-, and extensional-mode resonators have been studied to enhance the mass sensing performance in viscous media. Thanks to the ultra-high mass sensitivities (typically ~Hz/pg) and mass resolution (pg to fg), trace gas molecules and biological species using integrated resonant mass sensors have been demonstrated. More attention still needs to be made to tackle the challenges of detecting VHF/UHF resonances with picometer displacement sensitivity in air and liquid, such that the nanoresonators (including nanocantilevers and those made of low dimensional materials [14,69,72,73] can be widely used for bio/chemical sensing applications in gas and liquid-phases. In summary, the resonant MEMS/NEMS gravimetric sensors hold promise to continuously push the bio/chemical detection limits and bring a better understanding of gas/nanomaterial interaction and molecular binding mechanisms.

**Author Contributions:** H.J. prepared the manuscript. P.X. and X.L. reviewed and edited the manuscript. All authors have read and agreed to the published version of the manuscript.

**Funding:** The authors acknowledge funding support from the National Key R&D Program of China (2020YFB2008603), Shanghai Pujiang Program (20PJ1415600), Key Research Program of Frontier Sciences of the Chinese Academy of Sciences (QYZDJ-SSW-JSC001), Shanghai “Road and Belt” International Young Scientist Exchange Program (19510744600).

**Conflicts of Interest:** The authors declare no conflict of interest.

## References

1. Lavrik, N.V.; Sepaniak, M.J.; Datskos, P. Cantilever transducers as a platform for chemical and biological sensors. *Rev. Sci. Instrum.* **2004**, *75*, 2229–2253. [[CrossRef](#)]
2. Arlett, J.; Myers, E.; Roukes, M. Comparative advantages of mechanical biosensors. *Nat. Nanotechnol.* **2011**, *6*, 203–215. [[CrossRef](#)]
3. Johnson, B.N.; Mutharasan, R. Biosensing using dynamic-mode cantilever sensors: A review. *Biosens. Bioelectron.* **2012**, *32*, 1–18. [[CrossRef](#)]
4. Fritz, J.; Baller, M.K.; Lang, H.P.; Rothuizen, H.; Vettiger, P.; Meyer, E.; Güntherodt, H.-J.; Gerber, C.; Gimzewski, J.K. Translating biomolecular recognition into nanomechanics. *Science* **2000**, *288*, 316–318. [[CrossRef](#)] [[PubMed](#)]
5. Thundat, T.; Wachter, E.A.; Sharp, S.L.; Warmack, R.J. Detection of mercury vapor using resonating microcantilevers. *Appl. Phys. Lett.* **1995**, *66*, 1695–1697. [[CrossRef](#)]
6. Li, X.; Lee, D.-W. Integrated microcantilevers for high-resolution sensing and probing. *Meas. Sci. Technol.* **2011**, *23*, 022001. [[CrossRef](#)]
7. Ono, T.; Li, X.; Miyashita, H.; Esashi, M. Mass sensing of adsorbed molecules in sub-picogram sample with ultrathin silicon resonator. *Rev. Sci. Instrum.* **2003**, *74*, 1240–1243. [[CrossRef](#)]
8. Ekinici, K.L.; Huang, X.M.H.; Roukes, M.L. Ultrasensitive nanoelectromechanical mass detection. *Appl. Phys. Lett.* **2004**, *84*, 4469–4471. [[CrossRef](#)]
9. Dohn, S.; Sandberg, R.K.; Svendsen, W.E.; Boisen, A. Enhanced functionality of cantilever based mass sensors using higher modes. *Appl. Phys. Lett.* **2005**, *86*, 233501. [[CrossRef](#)]
10. Ilic, B.; Yang, Y.; Aubin, K.; Reichenbach, R.; Krylov, S.; Craighead, H.G. Enumeration of DNA molecules bound to a nanomechanical oscillator. *Nano Lett.* **2005**, *5*, 925–929. [[CrossRef](#)]
11. Nishio, M.; Sawaya, S.; Akita, S.; Nakayama, Y. Carbon nanotube oscillators toward zeptogram detection. *Appl. Phys. Lett.* **2005**, *86*, 133111. [[CrossRef](#)]
12. Yang, Y.T.; Callegari, C.; Feng, X.L.; Ekinici, K.L.; Roukes, M.L. Zeptogram-scale nanomechanical mass sensing. *Nano Lett.* **2006**, *6*, 583–586. [[CrossRef](#)] [[PubMed](#)]
13. Jensen, K.H.; Kim, K.; Zettl, A. An atomic-resolution nanomechanical mass sensor. *Nat. Nanotechnol.* **2008**, *3*, 533–537. [[CrossRef](#)]
14. Lassagne, B.; Garcia-Sanchez, D.; Aguasca, A.; Bachtold, A. ultrasensitive mass sensing with a nanotube electromechanical resonator. *Nano Lett.* **2008**, *8*, 3735–3738. [[CrossRef](#)]
15. Naik, A.; Hanay, M.S.; Hiebert, W.K.; Feng, X.L.; Roukes, M.L. Towards single-molecule nanomechanical mass spectrometry. *Nat. Nanotechnol.* **2009**, *4*, 445–450. [[CrossRef](#)]
16. Chaste, J.; Eichler, A.; E. Moser, J.; Ceballos, G.; Rurali, R.; Bachtold, A. A nanomechanical mass sensor with yoctogram resolution. *Nat. Nanotechnol.* **2012**, *7*, 301–304. [[CrossRef](#)]
17. Jin, D.; Li, X.; Bao, H.; Zhang, Z.; Wang, Y.; Yu, H.; Zuo, G. Integrated cantilever sensors with a torsional resonance mode for ultrasoluble on-the-spot bio/chemical detection. *Appl. Phys. Lett.* **2007**, *90*, 041901. [[CrossRef](#)]
18. Yu, H.; Li, X.; Gan, X.; Liu, Y.; Liu, X.; Xu, P.; Li, J.; Liu, M. Resonant-cantilever bio/chemical sensors with an integrated heater for both resonance exciting optimization and sensing repeatability enhancement. *J. Micromech. Microeng.* **2009**, *19*, 045023. [[CrossRef](#)]

19. Cai, S.; Li, W.; Xu, P.; Xia, X.; Yu, H.; Zhang, S.; Li, X. In situ construction of metal-organic framework (MOF) UiO-66 film on parylene-patterned resonant microcantilever for trace organophosphorus molecules detection. *Analyst* **2019**, *144*, 3729–3735. [[CrossRef](#)]
20. Yu, F.; Wang, J.; Xu, P.; Li, X. A tri-beam dog-bone resonant sensor with high-Q in liquid for disposable test-strip detection of analyte droplet. *J. Microelectromech. Syst.* **2016**, *25*, 244–251. [[CrossRef](#)]
21. Mehdizadeh, E.; Chapin, J.; Gonzales, J.; Rahafrooz, A.; Abdolvand, R.; Purse, B.; Pourkamali, S.; Chapin, J. Direct detection of biomolecules in liquid media using piezoelectric rotational mode disk resonators. In Proceedings of the 2012 IEEE Sensors, Taipei, Taiwan, 28–31 October 2012; pp. 1–4. [[CrossRef](#)]
22. Xia, X.; Zhang, Z.; Li, X. A Latin-cross-shaped integrated resonant cantilever with second torsion-mode resonance for ultra-resoluble bio-mass sensing. *J. Micromech. Microeng.* **2008**, *18*, 035028. [[CrossRef](#)]
23. Hwang, K.S.; Lee, J.H.; Park, J.; Yoon, D.S.; Park, J.H.; Kim, T.S. In-situ quantitative analysis of a prostate-specific antigen (PSA) using a nanomechanical PZT cantilever. *Lab Chip* **2004**, *4*, 547–552. [[CrossRef](#)]
24. Kwon, T.Y.; Eom, K.; Park, J.H.; Yoon, D.S.; Kim, T.S.; Lee, H.L. In situ real-time monitoring of biomolecular interactions based on resonating microcantilevers immersed in a viscous fluid. *Appl. Phys. Lett.* **2007**, *90*, 223903. [[CrossRef](#)]
25. Kwon, T.; Eom, K.; Park, J.; Yoon, D.S.; Lee, H.L.; Kim, T.S. Micromechanical observation of the kinetics of biomolecular interactions. *Appl. Phys. Lett.* **2008**, *93*, 173901. [[CrossRef](#)]
26. Tao, Y.; Li, X.; Xu, T.; Yu, H.; Xiong, B.; Wei, C. Resonant cantilever sensors operated in a high-Q in-plane mode for real-time bio/chemical detection in liquids. *Sens. Actuators B Chem.* **2011**, *157*, 606–614. [[CrossRef](#)]
27. Jin, D.; Li, X.; Liu, J.; Zuo, G.; Wang, Y.; Liu, M.; Yu, H. High-mode resonant piezoresistive cantilever sensors for tens-femtogram resolvable mass sensing in air. *J. Micromech. Microeng.* **2006**, *16*, 1017–1023. [[CrossRef](#)]
28. Xia, X.; Li, X. Resonance-mode effect on microcantilever mass-sensing performance in air. *Rev. Sci. Instrum.* **2008**, *79*, 074301. [[CrossRef](#)] [[PubMed](#)]
29. Yu, F.; Yu, H.; Xu, P.; Li, X. Precise extension-mode resonant sensor with uniform and repeatable sensitivity for detection of ppm-level ammonia. *J. Micromech. Microeng.* **2014**, *24*, 045005. [[CrossRef](#)]
30. Ekinci, K.L.; Yang, Y.T.; Roukes, M.L. Ultimate limits to inertial mass sensing based upon nanoelectromechanical systems. *J. Appl. Phys.* **2004**, *95*, 2682–2689. [[CrossRef](#)]
31. Ghatkesar, M.K.; Barwich, V.; Braun, T.; Ramseyer, J.-P.; Gerber, C.; Hegner, M.; Lang, H.P.; Drechsler, U.; Despont, M. Higher modes of vibration increase mass sensitivity in nanomechanical microcantilevers. *Nanotechnology* **2007**, *18*, 445502. [[CrossRef](#)]
32. Jia, H.; Lee, J.; Wang, Z.; Feng, P.X.-L. High-frequency SiC microdisk resonators operating in water with responses to H<sub>2</sub>O<sub>2</sub> and NH<sub>4</sub>OH. In Proceedings of the 2014 IEEE International Frequency Control Symposium (FCS), IEEE, Taipei, Taiwan, 19–22 May 2014; pp. 1–4. [[CrossRef](#)]
33. Jia, H.; Wu, X.; Tang, H.; Lu, Z.-R.; Feng, P.X.-L. Culturing and probing physical behavior of individual breast cancer cells on SiC microdisk resonators. In Proceedings of the 2015 IEEE International Conference on Micro Electro Mechanical Systems (MEMS), Estoril, Portugal, 18–22 January 2015; pp. 698–701. [[CrossRef](#)]
34. Jia, H.; Lu, X.; Main, C.; Lin, Q.; Feng, P.X.-L. Mode-dependent anchor loss in silicon carbide micromechanical disk resonators. In Proceedings of the 2019 Joint Conference of the IEEE International Frequency Control Symposium and European Frequency and Time Forum (EFTF/IFC), Orlando, FL, USA, 14–18 April 2019; pp. 1–2. [[CrossRef](#)]
35. Chen, H.; Jia, H.; Zorman, C.A.; Feng, P.X.L. Determination of elastic modulus of silicon carbide (SiC) thin diaphragms via mode-dependent Duffing non-linear resonances. *J. Microelectromech. Syst.* **2020**, *29*, 783–789. [[CrossRef](#)]
36. Jia, H.; Feng, P.X.-L. Very high-frequency silicon carbide microdisk resonators with multimode responses in water for particle sensing. *J. Microelectromech. Syst.* **2019**, *28*, 941–953. [[CrossRef](#)]
37. Jia, H.; Feng, P.X.-L. Tracing and resolving microparticle aquatic mass motion and distribution on multimode silicon carbide microdisk resonators. In Proceedings of the 2019 IEEE 32nd International Conference on Micro Electro Mechanical Systems (MEMS), Seoul, Korea, 27–31 January 2019; pp. 529–532. [[CrossRef](#)]
38. Liu, Y.; Li, X.; Zhang, Z.; Zuo, G.; Cheng, Z.; Yu, H. Nanogram per milliliter-level immunologic detection of alpha-fetoprotein with integrated rotating-resonance microcantilevers for early-stage diagnosis of hepatocellular carcinoma. *Biomed. Microdevices* **2008**, *11*, 183–191. [[CrossRef](#)] [[PubMed](#)]
39. Xu, T.; Yu, H.; Xu, P.; Xu, W.; Chen, W.; Chen, C.; Li, X. Real-time enzyme-digesting identification of double-strand DNA in a resonance-cantilever embedded microchamber. *Lab Chip* **2014**, *14*, 1206–1214. [[CrossRef](#)]
40. Beardslee, L.A.; Addous, A.M.; Heinrich, S.; Josse, F.; Dufour, I.; Brand, O. Thermal excitation and piezoresistive detection of cantilever in-plane resonance modes for sensing applications. *J. Microelectromech. Syst.* **2010**, *19*, 1015–1017. [[CrossRef](#)]
41. Yu, F.; Xu, P.; Wang, J.; Li, X. Length-extensional resonating gas sensors with IC-foundry compatible low-cost fabrication in non-SOI single-wafer. *Microelectron. Eng.* **2015**, *13*, 1–7. [[CrossRef](#)]
42. Xu, P.; Yu, H.; Li, X. Functionalized mesoporous silica for microgravimetric sensing of trace chemical vapors. *Anal. Chem.* **2011**, *83*, 3448–3454. [[CrossRef](#)]
43. Xu, P.; Li, X.; Yu, H.; Liu, M.; Li, J. Self-assembly and sensing-group graft of pre-modified CNTs on resonant micro-cantilevers for specific detection of volatile organic compound vapors. *J. Micromech. Microeng.* **2010**, *20*, 115003. [[CrossRef](#)]
44. Xu, P.; Yu, H.; Li, X. In situ growth of noble metal nanoparticles on graphene oxide sheets and direct construction of functionalized porous-layered structure on gravimetric microsensors for chemical detection. *Chem. Commun.* **2012**, *48*, 10784–10786. [[CrossRef](#)]

45. Xu, P.; Guo, S.; Yu, H.; Li, X. Mesoporous silica nanoparticles (MSNs) for detoxification of hazardous organophorous chemicals. *Small* **2014**, *10*, 2404–2412. [[CrossRef](#)]
46. Guo, S.; Xu, P.; Yu, H.; Li, X.; Cheng, Z. Hyper-branch sensing polymer batch self-assembled on resonant micro-cantilevers with a coupling-reaction route. *Sens. Actuators B Chem.* **2015**, *209*, 943–950. [[CrossRef](#)]
47. Guo, S.; Xu, P.; Yu, H.; Cheng, Z.; Li, X. Synergistic improvement of gas sensing performance by micro-gravimetrically extracted kinetic/thermodynamic parameters. *Anal. Chim. Acta* **2015**, *863*, 49–58. [[CrossRef](#)] [[PubMed](#)]
48. Yu, H.; Yang, T.; Chen, Y.; Xu, P.; Lee, D.-W.; Li, X. Chemo-mechanical joint detection with both dynamic and static microcantilevers for interhomologue molecular identification. *Anal. Chem.* **2012**, *84*, 6679–6685. [[CrossRef](#)] [[PubMed](#)]
49. Yu, H.; Xu, P.; Lee, D.-W.; Li, X. Porous-layered stack of functionalized AuNP-rGO (gold nanoparticles-reduced graphene oxide) nanosheets as a sensing material for the micro-gravimetric detection of chemical vapor. *J. Mater. Chem. A* **2013**, *1*, 4444–4450. [[CrossRef](#)]
50. Xia, X.; Guo, S.; Zhao, W.; Xu, P.; Yu, H.; Xu, T.; Li, X. Carboxyl functionalized gold nanoparticles in situ grown on reduced graphene oxide for micro-gravimetric ammonia sensing. *Sens. Actuators B Chem.* **2014**, *202*, 846–853. [[CrossRef](#)]
51. Liu, M.; Guo, S.; Xu, P.; Yu, H.; Xu, T.; Zhang, S.; Li, X. Revealing humidity-enhanced NH<sub>3</sub> sensing effect by using resonant microcantilever. *Sens. Actuators B Chem.* **2018**, *257*, 488–495. [[CrossRef](#)]
52. Lv, Y.; Yu, H.; Xu, P.; Xu, J.; Li, X. Metal organic framework of MOF-5 with hierarchical nanopores as micro-gravimetric sensing material for aniline detection. *Sens. Actuators B Chem.* **2018**, *256*, 639–647. [[CrossRef](#)]
53. Xu, T.; Xu, P.; Zheng, D.; Yu, H.; Li, X. Metal-organic frameworks for resonant-gravimetric detection of trace-level xylene molecules. *Anal. Chem.* **2016**, *88*, 12234–12240. [[CrossRef](#)] [[PubMed](#)]
54. Lv, Y.; Xu, P.; Yu, H.; Xu, J.; Li, X. Ni-MOF-74 as sensing material for resonant-gravimetric detection of ppb-level CO. *Sens. Actuators B Chem.* **2018**, *262*, 562–569. [[CrossRef](#)]
55. Wang, X.; Yao, F.; Xu, P.; Li, M.; Yu, H.; Li, X. Quantitative structure-activity relationship of nanowire adsorption to SO<sub>2</sub> revealed by in situ TEM technique. *Nano Lett.* **2021**, *21*, 1679–1687. [[CrossRef](#)]
56. Yu, H.; Xu, P.; Xia, X.; Lee, D.-W.; Li, X. Micro-/nanocombined gas sensors with functionalized mesoporous thin film self-assembled in batches onto resonant cantilevers. *IEEE Trans. Ind. Electron.* **2011**, *59*, 4881–4887. [[CrossRef](#)]
57. Xu, T.; Yu, H.; Xu, P.; Li, X. A chelating-bond breaking and re-linking technique for rapid re-immobilization of immune micro-sensors. *Biomed. Microdevices* **2011**, *14*, 303–311. [[CrossRef](#)] [[PubMed](#)]
58. Olcum, S.; Cermak, N.; Wasserman, S.C.; Christine, K.S.; Atsumi, H.; Payer, K.R.; Shen, W.; Lee, J.; Belcher, A.M.; Bhatia, S.N.; et al. Weighing nanoparticles in solution at the attogram scale. *Proc. Natl. Acad. Sci. USA* **2014**, *111*, 1310–1315. [[CrossRef](#)] [[PubMed](#)]
59. Lee, J.; Shen, W.; Payer, K.; Burg, T.P.; Manalis, S.R. Toward attogram mass measurements in solution with suspended nanochannel resonators. *Nano Lett.* **2010**, *10*, 2537–2542. [[CrossRef](#)]
60. Godin, M.; Delgado, F.F.; Son, S.; Grover, W.H.; Bryan, A.K.; Tzur, A.; Jorgensen, P.; Payer, K.; Grossman, A.D.; Kirschner, M.W.; et al. Using buoyant mass to measure the growth of single cells. *Nat. Methods* **2010**, *7*, 387–390. [[CrossRef](#)]
61. Olcum, S.; Cermak, N.; Wasserman, S.C.; Payer, K.; Shen, W.; Lee, J.; Manalis, S.R. Suspended nanochannel resonators at attogram precision. In Proceedings of the 2014 IEEE International Conference on Micro Electro Mechanical Systems (MEMS), San Francisco, CA, USA, 26–30 January 2014; pp. 116–119. [[CrossRef](#)]
62. Barton, R.A.; Ilic, B.; Verbridge, S.S.; Cipriany, B.R.; Parpia, J.M.; Craighead, H.G. Fabrication of a nanomechanical mass sensor containing a nanofluidic channel. *Nano Lett.* **2010**, *10*, 2058–2063. [[CrossRef](#)] [[PubMed](#)]
63. Burg, T.P.; Mirza, A.R.; Milovic, N.; Tsau, C.H.; Popescu, G.A.; Manalis, S.R.; Foster, J.S. Vacuum-packaged suspended microchannel resonant mass sensor for biomolecular detection. *J. Microelectromech. Syst.* **2006**, *15*, 1466–1476. [[CrossRef](#)]
64. Cermak, N.; Olcum, S.; Delgado, F.F.; Wasserman, S.C.; Payer, K.R.; A. Murakami, M.; Knudsen, S.M.; Kimmerling, R.J.; Stevens, M.M.; Kikuchi, Y.; et al. High-throughput measurement of single-cell growth rates using serial microfluidic mass sensor arrays. *Nat. Biotechnol.* **2016**, *34*, 1052–1059. [[CrossRef](#)]
65. Yu, H.; Chen, Y.; Xu, P.; Xu, T.; Bao, Y.; Li, X.  $\mu$ -‘Diving suit’ for liquid-phase high-Q resonant detection. *Lab Chip* **2016**, *16*, 902–910. [[CrossRef](#)]
66. Wang, X.; Cheng, Y.; Cai, S.; Chen, J.; Xu, P.; Chen, Y.; Yu, H.; Xu, T.; Zhang, S.; Li, X. Resonant-cantilever-detected kinetic/thermodynamic parameters for aptamer-ligand binding on a liquid-solid interface. *Anal. Chem.* **2020**, *92*, 11127–11134. [[CrossRef](#)]
67. Vancura, C.; Li, Y.; Lichtenberg, J.; Kirstein, K.U.; Hierlemann, A.; Josse, F. Liquid-phase chemical and biochemical detection using fully integrated magnetically actuated complementary metal oxide semiconductor resonant cantilever sensor systems. *Anal. Chem.* **2007**, *79*, 1646–1654. [[CrossRef](#)]
68. Li, Y.; Vancura, C.; Kirstein, K.-U.; Lichtenberg, J.; Hierlemann, A. monolithic resonant-cantilever-based CMOS microsystem for biochemical sensing. *IEEE Trans. Circuits Syst. I Regul. Pap.* **2008**, *55*, 2551–2560. [[CrossRef](#)]
69. Chiu, H.-Y.; Hung, P.; Postma, H.W.C.; Bockrath, M. Atomic-scale mass sensing using carbon nanotube resonators. *Nano Lett.* **2008**, *8*, 4342–4346. [[CrossRef](#)] [[PubMed](#)]
70. Li, M.; Tang, H.X.; Roukes, M.L. Ultra-sensitive NEMS-based cantilevers for sensing, scanned probe and very high-frequency applications. *Nat. Nanotechnol.* **2007**, *2*, 114–120. [[CrossRef](#)] [[PubMed](#)]
71. Yang, Y.; Xia, X.; Gan, X.; Xu, P.; Yu, H.; Li, X. Nano-thick resonant cantilevers with a novel specific reaction-induced frequency-increase effect for ultra-sensitive chemical detection. *J. Micromech. Microeng.* **2010**, *20*, 055022. [[CrossRef](#)]

- 
72. Jia, H.; Yang, R.; Nguyen, A.E.; Alvillar, S.N.; Empante, T.; Bartels, L.; Feng, P.X.-L. Large-scale arrays of single- and few-layer MoS<sub>2</sub> nanomechanical resonators. *Nanoscale* **2016**, *8*, 10677–10685. [[CrossRef](#)] [[PubMed](#)]
  73. Wang, Z.; Jia, H.; Zheng, X.-Q.; Yang, R.; Ye, G.; Chen, X.; Feng, P.X.-L. Resolving and tuning mechanical anisotropy in black phosphorus via nanomechanical multimode resonance spectromicroscopy. *Nano Lett.* **2016**, *16*, 5394–5400. [[CrossRef](#)] [[PubMed](#)]